MONITORING OF ARTIFICIAL RESERVOIR INDUCED LANDSLIDES FROM SPACE: A CASE STUDY OF FROM INDIA

Vishal Mishra[1*] ,Chandrahas Singh [1] , Kamal Jain [1,2]

[1] Dept. of Civil Engineering, Indian Institute of Technology Roorkee, 247667 Roorkee, India - (vmishra1, chandrahas,)@ce.iitr.ac.in
[2] Centre of Excellence Disaster Mitigation and Management, Indian Institute of Technology Roorkee, 247667 Roorkee, India - kjainfce@iitr.ac.in

KEY WORDS: Reservoir-induced-Landslides; Atmospheric Phase Screen; Sentinel-1;Google Earth Engine; Tropical Rainfall Measuring Mission (TRMM).

ABSTRACT:

Monitoring Reservoir-induced landslides is critical for determining and mitigating the geo-environmental risks associated with the artificial reservoir. This paper employs Persistent Scatterer Interferometry (PSI) technique for the mapping and monitoring of Reservoir Induced Landslides in the rim area of Baglihar Dam Reservoir on Chenab river (Jammu and Kashmir, India) along National Highway NH-244. It has been evident that the slope movements are necessarily impacted by the reservoir drawdown effect (RDE) as well as the rainfall. We have utilised 46 Sentinel-1A C-band radar satellite imagery of the study area. The monitoring results have yielded the Line of Sight slope movement along the reservoir rim varies from -97 mm/year to +80 mm/year. The temporal correlation between the displacements and the local precipitation (derived from TRMM using Google Earth Engine) was qualitatively analysed. Two unstable slopes have been identified and monitored.

1. INTRODUCTION

1.1 General Instructions

Reservoir-induced Landslides are the major geohazards associated with the damming of rivers in mountainous terrain (Petley, 2013). They shorten the reservoir capacity, decrease the utility of dams and threaten the life and infrastructure situated on the banks as well as on the downstream of the reservoirs. Damming of rivers changes the groundwater conditions as well as alters the status of forces on the inundated reservoir slopes leading to decrease in stability of these slopes. Fragile geology also contributes to this. Many artificial reservoirs such as Vajont Dam reservoir (Italy) (Paronuzzi et al., 2013), Tehri Dam reservoir (India) (Sati et al., 2020), Three Gorges Reservoir (China) (Tang et al., 2019), Potrerillos Dam reservoir (Argentina) (Michoud et al., 2016), etc. are examples of the places where inundation of the reservoir slopes have caused landslides.

The monitoring and mapping of Reservoir Landslides becomes of utmost importance given the impact of hazards associated. These landslides are needed to be studied in detail. Geomatics techniques has been used for mapping and studying landslides (Casagli et al., 2017). Differenent Geomatics techniques such as GPS, Total stations, Laser Scanners, Radar sensors etc have been employed for studying Landslides. SAR Remote Sensing can provide a cheaper tool for this (Casagli et al., 2010, Scaioni et al., 2014; Casagli et al., 2017; Rehman et al., 2020). Differential interferometry SAR (DInSAR) has been used a lot for estimating land deformation (such as landslides) from space. The advantage of this technique is that they have high sampling points which makes them cheaper as well as there reach to the remote areas. This techniques were limited by atmospheric noises, temporal disturbances and errors induced by external Digital Elevation Model (DEM). This bottleneck was addressed by the advent of Advanced DInSAR(A-DInSAR) techniques.
A-DInSAR techniques utilises stack of SAR Single Look SLC images for retrieving the deformation trend. The utilisation of time-series of data helps in mitigating the atmospheric noise. A-DInSAR techniques has been used for monitoring extremely slow to very slow movements (Lu et al., 2012). The advantages of employing Advanced DInSAR techniques for monitoring slow and very slow moving landslides are cost, weather independence, high spatial resolution, and the ability to visit isolated areas. The A-DInSAR approach has been frequently used to investigate reservoir-induced landslides (Wang et al., 2013; Neelmeijeret al., 2018; Zhao et al., 2018; Dini et al., 2020). One of the widely studied area with A-DInSAR techniques is Three Gorges Reservoir area (Liu et al.,2013; Tantianuparp et al., 2013; Shi et al., 2015).

Himalayan region is being developed and urbanised. The hydropower of the Himalayan rivers are being harnessed by damming them. This is leading to the development of many artificial reservoirs in Himalayas which have fragile geology and are tectonically active. One such reservoir is Baglihar Dam reservoir which has been studied by very few researchers (Singh et al., 2012). Many incidents of Landslides have taken place since the commencement of Hydroelectric Project.

The objective of this study to monitor the area for the movement on the reservoir rim slopes using ADInSAR or Persistent Scatterer Interferometry.

2. STUDY AREA

The Baglihar Dam Reservoir is situated in Indian administered territory of Jammu and Kashmir and it lies on the river Chenab. The area falls in the Lesser Himalayan region and is in seismic Zone IV. Construction of the dam had started in 1999. The study area is shown in Figure 1. Two National Highways: Jammu-Srinagar Highway (NH-44) and Batote-Doda-Kishtwar National Highway (NH-1B/ NH 244) the only road link of Doda and Kishtwar, pass through the study area.. Dam site lies on river Chenab between Batote town and Ramban near Pira on the NH44 whereas the NH 1B runs along the Reservoir.

*Corresponding Author

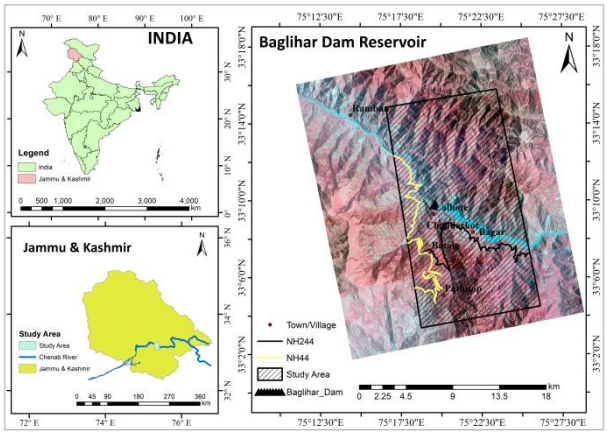

Figure 1. Location of the study area.

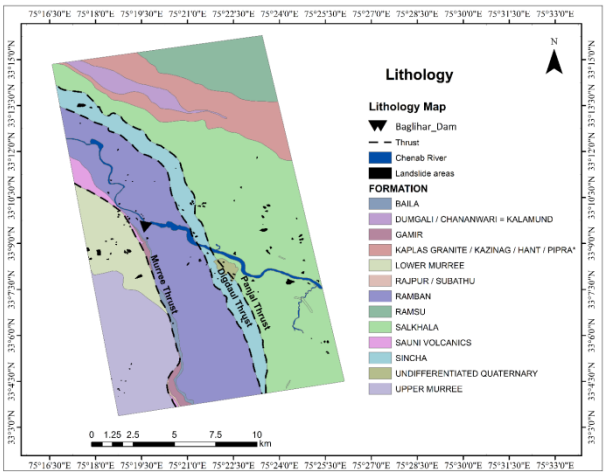

Figure 2. Lithology of the Study area

2.1 Geology

The study area comprises of metamorphic rocks which are highly sheared and foliated. Three thrusts lies in the study area namely Panjal, Digdaul and Murree. Panjal and Digdaul thrusts are situated in the northern and eastern parts of the study area where as Murree thrust lies to south of the dam. The hills of the study areaare highly dissected. Most of the mountains comprise hard rock, lime and gypsum stones as well as loose soil. the likelihood of reservoir water affecting these rocks is very high. The Sincha Formation, which is younger than the older Salkhala Formation in this region, is thrusted over by the older Salkhala Formation against Panjal Thrust. The landslide occurances and lithology is shown in the fig. 2. Figure 3 shows the Tectono-stratigraphic units within exposed in the study area (Singh et al., 2012).

3. DATA AND METHODOLOGY

3.1 Data

We have used a stack of 46 ascending Sentinel 1A-IW SLC images of VV polarisation of orbit. Specifications of the stack are illustrated in Table in Appendix with the master acquisition highlighted in red. Figure 3 also shows the characteristics of the data stack used in form of a histogram. The time-series is from November 2015 to January 2018, spanning over 27 months. Landslide Inventory was developed from the Geological Survey of India inventory as well as studying the Google Earth. The Tropical Rainfall Measuring Mission (TRMM) satellite data were extracted for the same time period using Google Earth Engine for estimating the daily precipitation over the study area.

Formation/Group	Lithology	Age
Recent Alluvium	Terrace deposits, hill wash scree, etc.,	Recent–Subrecent
Salkhala Group	*Malhori Phyllite Member* Consists of grey ferruginous phyllite,chlorite phyllite, slate or nearly quartzite *Baggar Schist Member* Consists of grey to dark coloured schists, at a few places garnetiferous	Proterozoic
	Panjal thrust	
Sincha	Quartzite, dolomite, limestone, phyllite slate, pebbly phyllite, diamictite	Proterozoic
	Unconformity	
Ramban	Slate, phyllite, quartzite and sandstone; gypsum lenses in basal part	Proterozoic
Baila	Carbonaceous phyllite, grey and whitish limestone, brecciated quartizite, argillite	Proterozoic
Gamir	Orthoquartzite , grit, shale, dolomite, limestone, etc.	Proterozoic
	Unconformity	
Souni Volcanics	Foliated and massive basic volcanics	Proterozoic
	Murree thrust	
Murree	Sandstone, claystone, shale, siltstone	Early Miocene to Oligocene

Figure 3. Tectono-stratigraphic units within exposed in the study area (Singh et al., 2012)

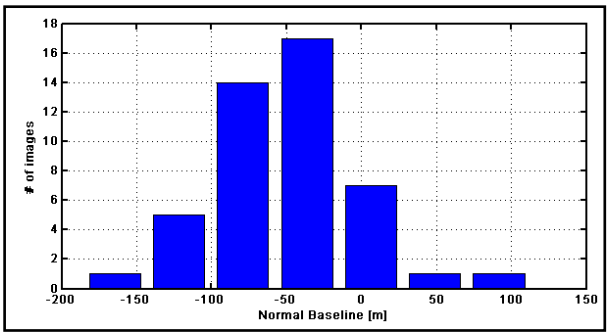

Figure 4. Characteristics of the Sentinel-1 datastack used in the study.

3.2 Methodology

Fig. 5 shows the general workflow followed in the study First the L1 Sentinel 1 IW data was downloaded. The data statistics were computed. Fig 6 shows the Spatio-temporal connection of different Sentinel-1 images. Precise orbit data was applied for the data stack.. Common area for processing was specified. It was followed by the step of images coregistration. In this step, offsets between the master and slaves is evaluated. This evaluation is done on the basis of amplitude information. Alignment of each slave image is done with the master image by resampling them with sub-pixel accuracy.

Multi Image reflectivity map was then generated (fig. 7). Reflectivity map is image where each pixel is the temporal mean of corresponding pixels from all the image in the resampled dataset. It is calculated using Equation (1):

$$m_A = \sum_{i=1}^{n} I_i / n \quad (1)$$

This map helps in identification of targets which have stable reflectivity behavior throughout the time-series dataset. The primary Permanent Scatterer candidates were chosen on behalf

of Amplitude Stability Index (ASI). (ASI) has been used for thresholding which is calculated as given in Equation (2) where σA and mA are the standard deviation and the average of the amplitude values respectively.

$$ASI = 1 - D_A = 1 - \frac{\sigma_A}{m_A} \quad (2)$$

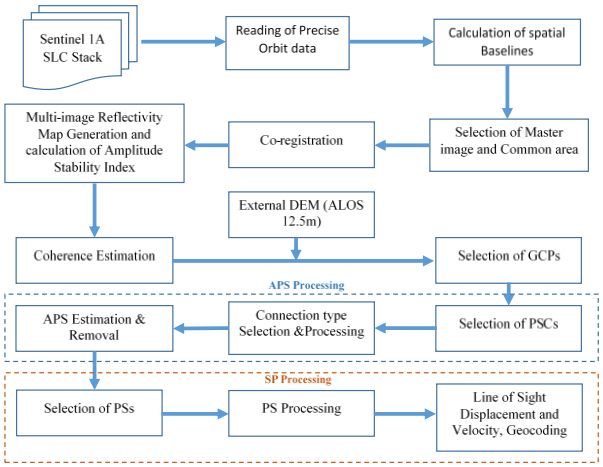

Figure 5. Methodology Flowchart

For this analysis, ASI threshold value has been chosen as 0.69 for the initial PS selection. Following the selection of the first order PS, a reference network was formed by Delaunay triangulating the PSs. Each edge of this network has its differential deformation velocity and differential residual topographic error (RTE) calculated. The estimated linear model (linear displacement velocities and residual height) is then subtracted, and the Atmospheric Phase Screen is calculated using graph inversion from the phase residuals. The velocity value of at least one pixel known as the reference point is kept as zero while performing Graph inversion.

Next phase of processing was sparse point processing or selection of second order PS. In this phase the thresholding was relaxed and the threshold value of ASI was selected as 0.6 in order to obtain a densified PS network. It was succeeded with APS removal. the APS removal was conducted using the same parameters and the reference point as for APS estimation in the prior steps. After the APS removal the displacement and thus velocity was estimated.

4. RESULTS AND DISCUSSIONS

Fig. 7 shows the reflectivity map in the SAR image coordinate. River Chenab is visible in the reflectivity map as the black snake like feature.

From the results (fig. 8) it can be inferred that the presence of active PS are more on the northern bank of reservoirs. There are many active PS present along the NH-244 (which going along the southern bank of the Reservoir). The field reports confirms that there are landslides happening on the southern rim of the Reservoir along NH-244 during the study period which has resulted in loss of coherence among the images thus less PS were detected on the southern side. Landslide or slope stability southern banks or left bank of the Reservoir (from the direction of flow) are of more concern as they endanger the National Highway passing through it which is the lifeline of the area. Northern banks are also very vulnerable. there have been many incidences of landslides occuring on these slopes. The slopes of the *nallah* or smaller stream entering into the Chenab from north near the dam are also active. The geology in the northern part of the study area belongs to the stable lithology and consists of stable PS (Figure 7).

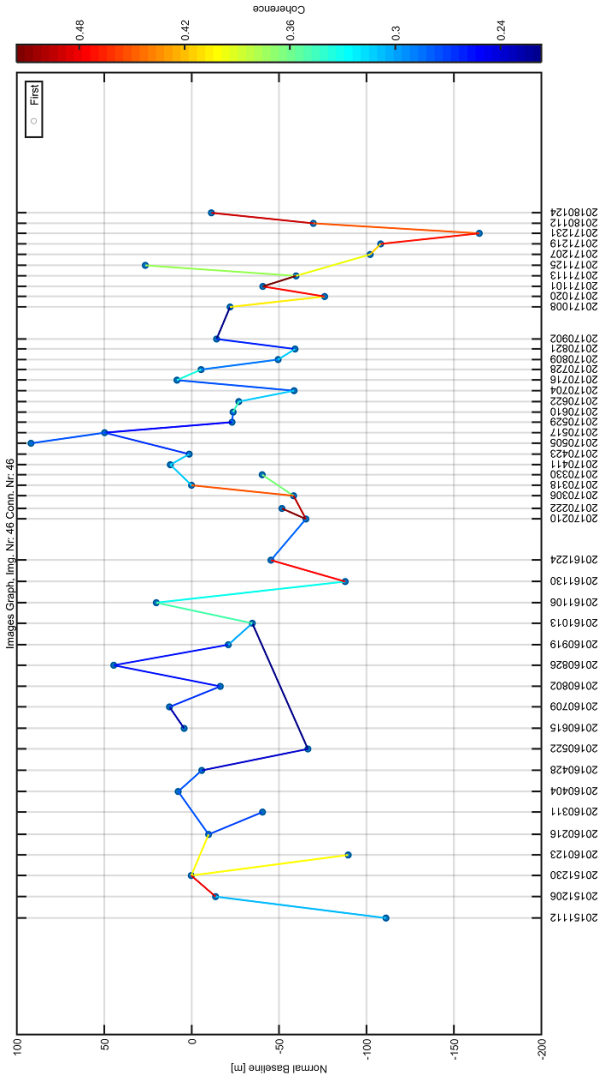

Figure 6. Spatio-temporal connection of different Sentinel-1 images.

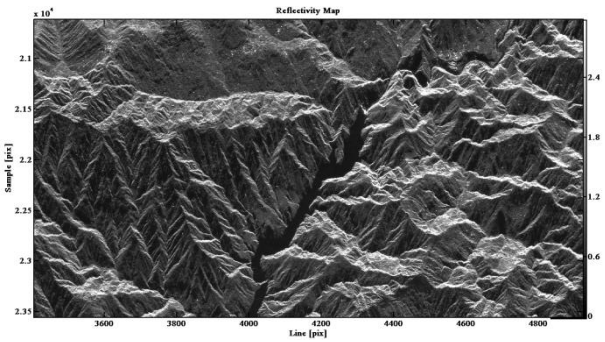

Figure 7. Reflectivity Map

The toe erosion is a common site on the inundated slopes of the reservoir. By observing the most of the active PS points, it can be inferred that slow movement was taking place between the time spanning from the months of November and subsequent January. Especially many points showed very slow movement between October 2016 to February 2017. This can also be attributed to a very low rainfall between this period as inferred from the TRMM derived precipitation data. Some old slides that occurred in 2011 has been stabilised.

In the fig. 9 the Landslide A is in the vicinity of the dam on the southern bank of the river near to the dam. It is 250 m wide with its toe submerged in the reservoir and crown is lying near the road. It is very old slide. Our PS analysis produced 21 points in this slide area. These PS are exhibiting deformation rate varying from -96.4 mm/year to 97.7 mm/year. On basis of stability only eight points of these were selected.. The points at the toe are showing very low velocities(< 10 mm/year). The fig. 10 shows the time series or trend of displacement of nine PS which are showing positive LoS velocity (depicted with blue in Figure 8) situated on the body of Landslide A. 8PS on the body of landslide A show a correlation between active period and precipitation and melting seasonal pattern. Between November '16 to February '17 the precipitation is very low (fig. 10) and the deformation of PSs are negligible.

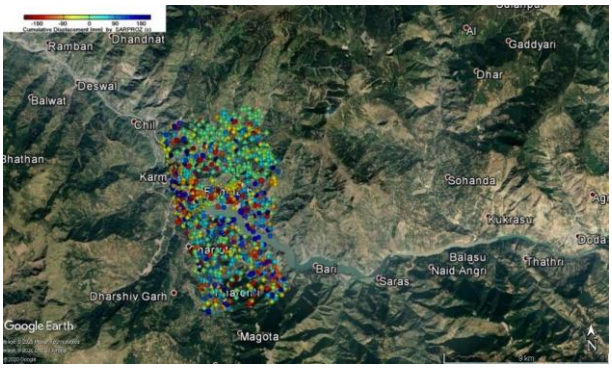

Figure 8. The PS obtained on the study area laid on the Google Earth classified according to its velocity. The green and yellow coloured PS are stable ones. The Northern part of the study area is a stable one. The southern part has three thrusts and is active. Two main highways pass through it; thus, it has many unstable points

Figure 9. Persistent Scatterers on a Landslide A on the Rim of the Reservoir. Red ones are showing negative LoS displacement whereas Blue ones are showing positive LoS movements

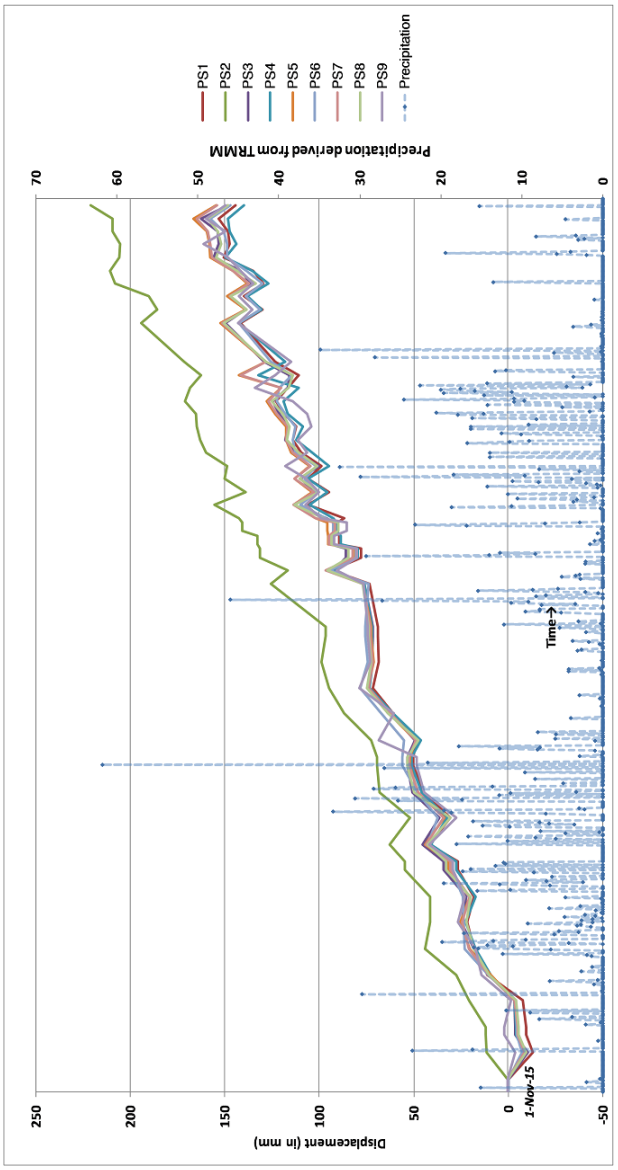

Figure 9. Displacement of Persistent Scatterers on Landslide A vs. Precipitation from TRMM.

5. CONCLUSION

Baglihar reservoir area is plagued with Reservoir induced landslides. The multi-temporal interferometric analysis has been successful in identifying and monitoring the unstable slopes in the Baglihar reservoir on both southern and northern part of the rim. The PSI can be helpful in modelling of Landslides using SAR images in data scares environment. The study has been limited due to two major factors which are the lack of in-situ displacement measurements for the validation and the presence of vegetation and water vapour in the area. Presence of vegetation induces deccorelation on temporal scale and makes the nalysis more challenging. This study helps in environmental assessment of impact of artificial reservoir on the submerged slopes and slopes in its vicinity. This analysis can be extended to multiple sensor analysis using TerraSAR-X, ENVISAT and other sensor data. This will provide a clear picture of the landslide activity in the stduy area. Also geophysical and geotechnical techniques can be applied to make the sllope stability analysis more extensive. Creep with dense vegetation is likely to go undetected due to InSAR coherence loss since C-

band data is easily decorrelated with the presence of vegetation. As a result, our findings could understate the true magnitude of active landslides in the studied area.

6. ACKNOWLEDGEMENTS

This work is supported by Ministry of Human Resource Development (Government of India) Scholarship. The dataset used in the study is Copernicus Sentinel-1 data for years 2015, 2016, 2017 and 2018, are retrieved from ASF DAAC. Data have been processed by SARPROZ (Copyright (c) 2009 Daniele Perissin, www.sarproz.com). We are grateful to Mr. Kapil Malik and SARPROZ team for giving an evaluation copy of the software tool. Authors would like to thank the Indian Institute of Technology Roorkee for providing resources..

7. REFERENCES

Casagli, N., Catani, F., del Ventisette, C., Luzi, G., 2010. Monitoring, prediction, and early warning using ground-based radar interferometry. Landslides 7, 291–301. https://doi.org/10.1007/s10346-010-0215-y

Casagli, N., Frodella, W., Morelli, S., Tofani, V., Ciampalini, A., Intrieri, E., Raspini, F., Rossi, G., Tanteri, L., Lu, P., 2017. Spaceborne, UAV and ground-based remote sensing techniques for landslide mapping, monitoring and early warning. Geoenvironmental Disasters 4. https://doi.org/10.1186/s40677-017-0073-1

Dini, B., Manconi, A., Loew, S., Chophel, J., 2020. The Punatsangchhu-I dam landslide illuminated by InSAR multitemporal analyses. Scientific Reports 10. https://doi.org/10.1038/s41598-020-65192-w.

Liu, P., Li, Z., Hoey, T., Kincal, C., Zhang, J., Zeng, Q., Muller, J.P., 2013. Using advanced inSAR time series techniques to monitor landslide movements in Badong of the Three Gorges region, China. International Journal of Applied Earth Observation and Geoinformation 21, 253–264. https://doi.org/10.1016/j.jag.2011.10.010

Lu, P., Casagli, N., Catani, F., Tofani, V., 2012. Persistent scatterers interferometry hotspot and cluster analysis (PSI-HCA) for detection of extremely slow-moving landslides. International Journal of Remote Sensing 33, 466–489. https://doi.org/10.1080/01431161.2010.536185

Michoud, C., Baumann, V., Lauknes, T.R., Penna, I., Derron, M.H., Jaboyedoff, M., 2016. Large slope deformations detection and monitoring along shores of the Potrerillos dam reservoir, Argentina, based on a small-baseline InSAR approach. Landslides 13, 451–465. https://doi.org/10.1007/s10346-015-0583-4

Neelmeijer, J., Schöne, T., Dill, R., Klemann, V., Motagh, M., 2018. Ground deformations around the Toktogul reservoir, Kyrgyzstan, from envisat ASAR and sentinel-1 data-A case study about the impact of atmospheric corrections on InSAR time series. Remote Sensing 10. https://doi.org/10.3390/rs10030462

Paronuzzi, P., Rigo, E., Bolla, A., 2013. Influence of filling-drawdown cycles of the Vajont reservoir on Mt. Toc slope stability. Geomorphology 191, 75–93. https://doi.org/10.1016/j.geomorph.2013.03.004

Petley, D., 2013. GLOBAL LOSSES FROM LANDSLIDES ASSOCIATED WITH DAMS AND RESERVOIRS. Italian Journal of Engineering Geology and Environment-Book Series. https://doi.org/10.4408/IJEGE.2013-06.B-05

Sati, S.P., Sharma, S., Sundriyal, Y.P., Rawat, D., Riyal, M., 2020. Geo-environmental consequences of obstructing the Bhagirathi River, Uttarakhand Himalaya, India. Geomatics, Natural Hazards and Risk 11, 887–905. https://doi.org/10.1080/19475705.2020.1756464

Scaioni, M., Longoni, L., Melillo, V., Papini, M., 2014. remote sensing Remote Sensing for Landslide Investigations: An Overview of Recent Achievements and Perspectives. Remote Sens 6, 1. https://doi.org/10.3390/rs60x000x

Shi, X., Zhang, L., Balz, T., Liao, M., 2015. Landslide deformation monitoring using point-like target offset tracking with multi-mode high-resolution TerraSAR-X data. ISPRS Journal of Photogrammetry and Remote Sensing 105, 128–140. https://doi.org/10.1016/j.isprsjprs.2015.03.017

Singh, Y., Bhat, G.M., Sharma, V., Pandita, S.K., Thakur, K.K., 2012. Reservoir induced landslide at Assar, Jammu and Kashmir: A case study. Journal of the Geological Society of India 80, 435–439. https://doi.org/10.1007/s12594-012-0162-4

Tang, H., Wasowski, J., Juang, C.H., 2019. Geohazards in the three Gorges Reservoir Area, China – Lessons learned from decades of research. Engineering Geology. https://doi.org/10.1016/j.enggeo.2019.105267

Tantianuparp, P., Shi, X., Zhang, L., Balz, T., Liao, M., 2013. Characterization of landslide deformations in three Gorges area using multiple inSAR data stacks. Remote Sensing 5, 2704–2719. https://doi.org/10.3390/rs5062704

Ur Rehman, M., Zhang, Y., Meng, X., Su, X., Catani, F., Rehman, G., Yue, D., Khalid, Z., Ahmad, S., Ahmad, I., 2020. Analysis of landslide movements using interferometric synthetic aperture radar: A case study in Hunza-Nagar Valley, Pakistan. Remote Sensing 12. https://doi.org/10.3390/RS12122054

Wang, G., Xie, M., Chai, X., Wang, L., Dong, C., 2013. D-InSAR-based landslide location and monitoring at Wudongde Hydropower Reservoir in China. Environmental Earth Sciences 69, 2763–2777. https://doi.org/10.1007/s12665-012-2097-x

Zhao, C., Kang, Y., Zhang, Q., Lu, Z., Li, B., 2018. Landslide identification and monitoring along the Jinsha River catchment (Wudongde reservoir area), China, using the InSAR method. Remote Sensing 10. https://doi.org/10.3390/rs10070993

8. APPENDIX

Date	Polari-sation	Normal Baseline (m)	Temporal Baseline (days)
12-Nov-15	VV	-111.1907	-492.00004
6-Dec-15	VV	-13.737559	-468.00004
30-Dec-15	VV	0.168597	-444.00005
23-Jan-16	VV	-89.58472	-420.00006
16-Feb-16	VV	-9.755637	-396.00007
11-Mar-16	VV	-40.586902	-372.00007
4-Apr-16	VV	7.662033	-348.00006
28-Apr-16	VV	-5.826533	-324.00005
22-May-16	VV	-66.520253	-300.00003
15-Jun-16	VV	4.253331	-276.00002
9-Jul-16	VV	12.632238	-252
2-Aug-16	VV	-16.431118	-227.99998
26-Aug-16	VV	44.500811	-203.99997
19-Sep-16	VV	-21.013528	-179.99996
13-Oct-16	VV	-34.74393	-155.99996
6-Nov-16	VV	20.160513	-131.99996
30-Nov-16	VV	-87.878355	-107.99996
24-Dec-16	VV	-45.395721	-83.999973
10-Feb-17	VV	-65.39115	-36.000001
22-Feb-17	VV	-51.682016	-24.000002
6-Mar-17	VV	-58.355744	-12.000003
18-Mar-17	VV	0	0
30-Mar-17	VV	-40.408005	12.000003
11-Apr-17	VV	12.138717	24.000009
23-Apr-17	VV	1.347793	36.000015
5-May-17	VV	91.855608	48.000024
17-May-17	VV	49.722669	60.000031
29-May-17	VV	-23.172186	72.000037
10-Jun-17	VV	-23.761315	84.000047
22-Jun-17	VV	-27.035556	96.000055
4-Jul-17	VV	-58.630608	108.000061
16-Jul-17	VV	8.355024	120.000069
28-Jul-17	VV	-5.448255	132.000079
9-Aug-17	VV	-49.479756	144.000086
21-Aug-17	VV	-59.177967	156.000092
2-Sep-17	VV	-14.325038	168.000098
8-Oct-17	VV	-22.001427	204.00011
20-Oct-17	VV	-76.09695	216.000112
1-Nov-17	VV	-40.771465	228.000112
13-Nov-17	VV	-59.749924	240.000108
25-Nov-17	VV	26.450639	252.000106
7-Dec-17	VV	-102.15817	264.000098
19-Dec-17	VV	-108.17333	276.000095
31-Dec-17	VV	-164.56003	288.000088
12-Jan-18	VV	-69.645751	300.000085
24-Jan-18	VV	-11.327517	312.00008